

RSC Advances



This is an *Accepted Manuscript*, which has been through the Royal Society of Chemistry peer review process and has been accepted for publication.

Accepted Manuscripts are published online shortly after acceptance, before technical editing, formatting and proof reading. Using this free service, authors can make their results available to the community, in citable form, before we publish the edited article. This *Accepted Manuscript* will be replaced by the edited, formatted and paginated article as soon as this is available.

You can find more information about *Accepted Manuscripts* in the [Information for Authors](#).

Please note that technical editing may introduce minor changes to the text and/or graphics, which may alter content. The journal's standard [Terms & Conditions](#) and the [Ethical guidelines](#) still apply. In no event shall the Royal Society of Chemistry be held responsible for any errors or omissions in this *Accepted Manuscript* or any consequences arising from the use of any information it contains.

Three-dimensional coordination polymers constructed from C_2 -symmetric linkers of pyridyl dicarboxylate ligands

Ruirui Yun*, Yaqin Jiang, Shizhong Luo, Cheng Chen

Abstract Two zinc(II) metal-organic frameworks (MOFs), $\{[Zn(L_1)]\cdot DMF\}_\infty$ (**1**) with tubular channels along a axis, and $\{[Zn(L_2)]\cdot DMF\}_\infty$ (**2**) with Zn-(COO)-Zn chains, have been constructed based on 5-(pyridin-4-yl)isophthalic acid (H_2L_1) and 4,4'-(pyridine-3,5-diyl)dibenzoic acid (H_2L_2) with Zn^{2+} , respectively. Both of the MOFs were characterized by IR spectroscopy, thermogravimetry, single crystal and powder X-ray diffraction methods. Network analysis reveals that **1** is 3,6-connected binodal net with the **rtl** topology and **2** forms a 5-connected uninodal net with the **bnn** topology. Additionally, the porosity of MOF **1** was confirmed by N_2 and CO_2 gas adsorption.

Introduction

The past two decades have witnessed the rapid development of metal-organic frameworks (MOFs), which constructed from organic ligands and metal center, due to their fantastic structures and various potential applications, such as in strategic storage and separation of gases, catalysis, chemical sensing and so on.¹ Recent years, we are interested in the design and synthesis of porous MOFs from large multidentate carboxylate linkers and paddle-wheel SBUs (second building units), because such an approach may facilitate the generation of high surface area MOFs.² To obtain fascinating MOFs, we introduced N-donor to the framework, which can change the coordination mode of the conventional pure carboxylate acid.³ As mentioned above, in recent years, we turn our attention to pyridyl-carboxylate ligands, and additionally, it is surprising that little investigation of pyridyl-carboxylate and elongated bridging pyridyl carboxylic acids have been undertaken in MOFs.⁴

The Key Laboratory of Functional Molecular Solids, Ministry of Education, Anhui Key Laboratory of Functional Molecular Solids, Anhui Laboratory of Molecule-Based Materials, College of Chemistry and Materials Science, Anhui Normal University, Wuhu 241000, People's Republic of China.

E-mail: yunruirui@gmail.com

To explore how the ligand size and its flexibility influence on the stability of materials. Herein, we reported two Zn-MOFs, which were $\{[Zn(L_1)]\cdot DMF\}_\infty$ (**1**) and $\{[Zn(L_2)]\cdot DMF\}_\infty$ (**2**) with Zn-(COO)-Zn chains, constructed by elongated pyridyl carboxylic acid ligands with one pyridyl donor and two carboxylic groups, namely as, 5-(pyridin-4-yl)isophthalic acid (H_2L_1) and 4,4'-(pyridine-3,5-diyl)-dibenzoic acid (H_2L_2).

Experimental section

General information

All Chemicals and solvents were of reagent grade and used as received without further purification. The ligand H_2L_1 was prepared according to the reference we previous reported and the method to synthesize H_2L_2 was placed in Supporting Information. The FT-IR spectra were recorded from KBr pellets in the range of 4000-400 cm^{-1} on a VECTOR 22 spectrometer. The elemental analysis was carried out with a Perkin-Elmer 240C elemental analyzer. Thermal analyses were performed on a Universal V3.9A TA Instruments from room temperature to 600°C with a heating rate of 10°C/min under flowing nitrogen. 1H NMR spectra were recorded on a Bruker DRX-500 spectrometer at ambient temperature with tetramethylsilane as an internal reference. The powder X-ray diffraction patterns (PXRD) measurements were carried on a Bruker axis D8 Advance 40kV, 40mA for $CuK\alpha$ ($\lambda = 1.5418 \text{ \AA}$) with a scan rate of 0.2 s/deg at room temperature.

Preparation of 1 and 2. A mixture of $ZnNO_3\cdot 6H_2O$

(29mg, 0.1mmol), H_2L_1 (6.2 mg, 0.025 mmol), HNO_3 (10 μ l, 16mol/L) and *N,N*-dimethylformamide (DMF) = 2 ml was stirred for ca. 10 min in air then transferred and sealed in a 20 ml Teflon-lined autoclave, which was heated at 85°C for 24h. After cooling to the room temperature, the colorless block crystals were obtained. Yield: 73% (based on H_2L_1). Anal. Calcd for evacuated samples of **1** ($C_{16}H_{14}ZnN_2O_5$): C, 50.61; H, 3.72; N, 7.38; Found: C, 50.92; H, 3.92; N, 7.59%. IR (cm^{-1} , KBr): 3433s, 2926m, 1673s, 1620vs, 1507m, 1441m, 1383vs, 1299 m, 1256w, 1223w, 1087m, 836w, 777m, 725m, 647w, 566w, 477w. **2** were obtained by the same condition except that H_2L_1 was placed by H_2L_2 , respectively. (**2** ($C_{22}H_{18}ZnN_2O_5$): C, 57.98; H, 3.98; N, 6.15; Found: C, 57.79; H, 3.61; N, 6.01).

Single crystal X-ray study

Single-crystal X-ray diffraction data were measured on a Bruker Smart Apex CCD diffractometer at 293 K using graphite monochromated $Mo/K\alpha$ radiation ($\lambda = 0.71073$ Å). Data reduction was made with the Bruker Saint program. The crystal of **1** and **2** were mounted in a flame sealed capillary, respectively, containing a small amount of mother liquor to prevent desolvation during data collection, and data were collected at 293K. The structures were solved by direct methods and refined with full-matrix least squares technique using the SHELXTL package.⁵ Non-hydrogen atoms were refined with anisotropic displacement parameters during the final cycles. Organic hydrogen atoms were placed in calculated positions with isotropic displacement parameters set to $1.2 \times U_{eq}$ of the attached atom. The hydrogen atoms of the ligand and water molecules could not be located, but are included in the formula. The unit cell of **2** include a large region of disordered solvent molecules, which could not be modeled as discrete atomic sites. The SQUEEZE subroutine of the PLATON software suite⁶ was applied to remove the scattering from the highly disordered solvent molecules due to the guest solvent molecules are highly disordered and impossible to refine using conventional discrete-atom models. Structure information of **1** and **2** were deposited at the Cambridge Crystallographic Data Center (CCDC reference numbers were: 946740 and 946741). Crystal data and further information on the structure determination are summarized in Table S1.

Sample activation

Supercritical carbon dioxide (SCD) activation method was used to remove guest solvent molecules from the MOFs. SCD processing was performed with a Tousimi Samdri PVT-30 critical point dryer. Before SCD drying, DMF-solvated MOF samples were soaked in ethanol for 3 days, with the soaking solution being replaced every 4 h. After soaking, the ethanol-containing samples were placed inside the dryer and the acetone was exchanged with CO_2 (liquid) over a period of 2 h. The temperature was then raised and CO_2 was vented under supercritical conditions. Before the measurements, the samples were treated by SCD. And then, the sample was evacuated at 30 °C for 12 h to remove the included solvent molecules and obtain an activated sample. Ultra-high-purity grade N_2 and CO_2 source were used in the sorption measurement.

Gas adsorption experiments

In the gas sorption measurements, all of the gases used are of 99.999% purity. Low-pressure N_2 (at 77 K) and CO_2 (273 K) adsorption measurements (up to 1 bar) were performed on Micromeritics ASAP 2020 M+C surface area analyzer. For all low-pressure isotherms, warm and cold free space correction measurements were performed using ultra-high-purity He gas (UHP grade 5.0, 99.999% purity).

Results and discussion

Crystal structure description

The asymmetric unit of **1** confirms the assignment of 1:1 stoichiometry for Zn(II) : L_1 (Fig. 1). Single crystal X-ray determination of **1** reveals that $\{[Zn(L_1)] \cdot DMF\}_\infty$ (**1**) crystallizes in monoclinic space group $P2_1/c$. The central Zn(II) ion is five-coordinated by four oxygen atoms and one pyridyl N-donor from five different Ligands in a square-pyramidal geometry. Four carboxylate groups from different ligands linked a pair of zinc ions to construct the paddlewheel units $[Zn_2(COO)_4N_2]$, in which the axial positions are occupied by two pyridyl N-donors from the other two different ligands.

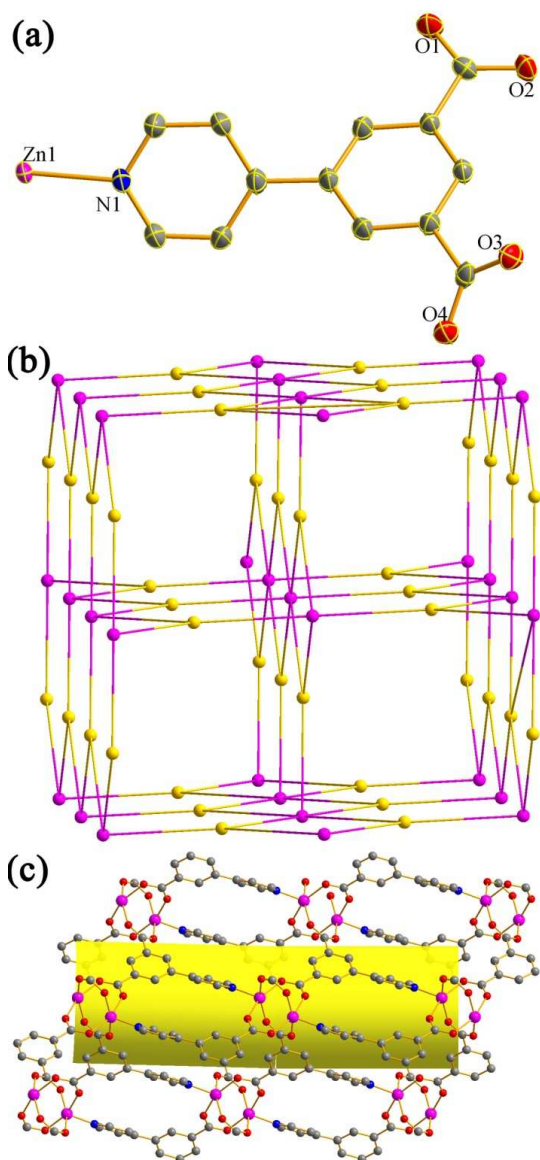


Fig. 1. (a) View of **1** with atom labeling of the Zn(II) coordination sphere and the asymmetric unit (lattice DMF molecule is omitted for clarity). Displacement ellipsoids are drawn at the 50 % probability level. (b) $(4\cdot6^2)_2(4^2\cdot6^{10}\cdot8^3)$ **rtl** type topological diagram (yellow: ligands, pink: paddlewheel nodes). (c) One tubular channel along *a* axis.

To get better insight into the intricate structure, a topological analysis was carried out. Considering the paddlewheel units are simplified as six-connected nodes and the ligand as three-connected linkers, the overall structure of **1** can be described as a two nodal (3,6)-connected net with the stoichiometry (3-c)₂(6-c). The point (Schäffli) symbol for **1** is $(4\cdot6^2)_2(4^2\cdot6^{10}\cdot8^3)$ as calculated using TOPOS.⁷ Consequently, the topology of

1 is assigned with RCSR symbol **rtl**.⁸ As shown in fig. 1, there exist nano-tubular channels with the ligand L_1 as the walls, extending infinitely along the *a* axis. The channels are filled of disorder DMF solvent molecules in the as-synthesized crystals of **1**. The accessible volume is 31% (657.6 Å³) per unit cell (2086.3 Å³) as calculated by PLATON.⁹

Comparing with the ligand of H_2L_1 , when the extending ligand H_2L_2 was used and the framework of **2** obtained. Single crystal X-ray diffraction analysis reveals that **2** crystallizes also in monoclinic $P2_1/c$ and its asymmetric unit consist of one Zn(II) center, one L_2 ligand and DMF solvent molecule (see Fig. 2). In this structure, the Zn(II) center adopts a nearly trigonal bipyramidal coordination geometry, which is provided by four oxygen atoms and one pyridyl N-donor from five different ligands.

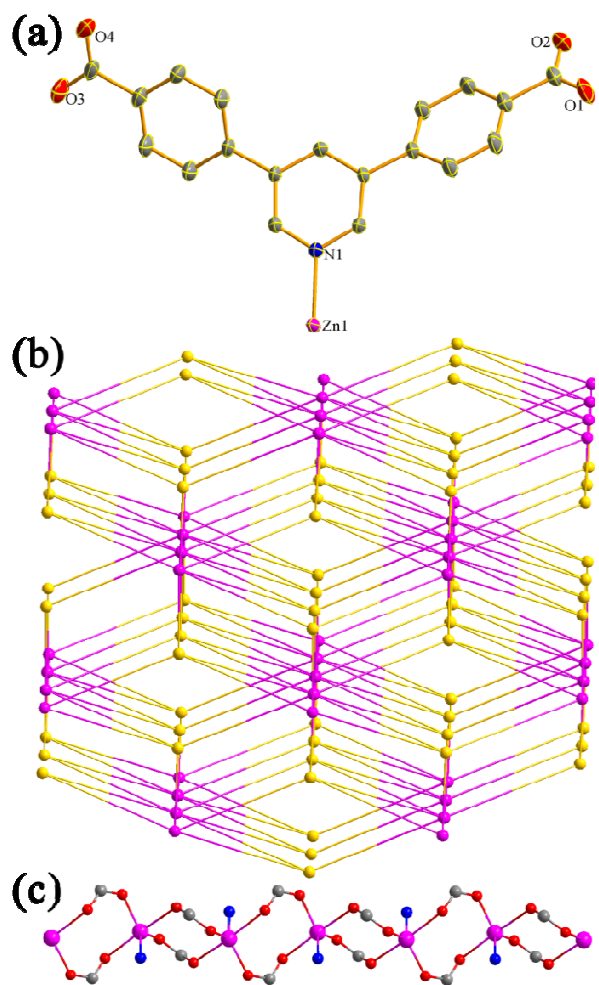


Fig. 2. (a) A view of **2** with atom labeling of the Zn(II) coordination sphere and the asymmetric unit (lattice DMF

molecule and hydrogen atoms are omitted for clarity). Displacement ellipsoids are drawn at the 50 % probability level. (b) $(4^6 \cdot 6^4)$ **bnn** type topological diagram (yellow: ligands, pink: metal center). (c) Zn-(COO)-Zn chains along *c* axis.

As shown in Fig. 2, considering both of the ligands and metal centers as five-connected nodes, the overall structure of **2** can be defined as uninodal five-connected net with the topology of **bnn** type which calculated by TOPOS. There exists Zn-(COO)-Zn chains along *c* axis, which are linked by ligand and further extend to three-dimensional framework.

Actually, the ligands of them are very similar, except the size of branch. However, the large size of H_2L_2 made it flexible, resulting in a much freer for rotating. For the reason we mentioned above, metal center of **2** was adopted to five-coordination with trigonal bipyramidal geometry, while Zn (II) in the structure of **1** was tetragonal pyramid with rigid coordination site.

Thermogravimetric Analysis

To study the frameworks stabilities of **1** and **2**, we performed thermogravimetric analysis (TGA) studies (Fig S3, ESI). The TGA curve of **1** displays steady weight loss in temperature range of 170-230 °C (ca. 21.2%), corresponding to the evacuation of the lattice DMF molecules (calc. 19.2%). The decomposition of the whole structure corresponds to the rapid weight loss in 260-270 °C. Because of the large size of ligand for **2**, the comparable large weight losses from 80-180 °C, it maybe due to the solvent on the surface and lattice solvents. No obvious weight losses occurred until approximately 330 for **2**, indicating that the decomposition of the whole structure from then on.

PXRD and gas adsorption properties

To confirm the permanent porosity of the MOFs, a large amount of pure **1** and **2** can be readily prepared. The purity of the materials is confirmed by PXRD analysis, in which the experimental PXRD pattern is well consistent with the one obtained from the simulated PXRD based on the single crystal samples at room temperature (Fig. S1, ESI). The as-synthesized samples were treated by SCD (supercritical carbon dioxide), and then the activated sample was degassed under high vacuum for 24 hours to obtain the evacuated framework.

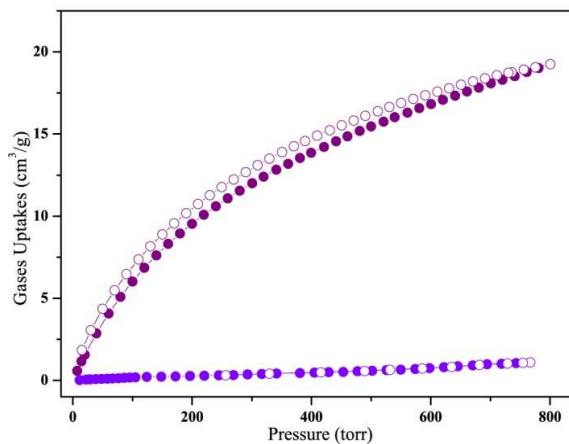


Fig. 3. Nitrogen (at 77 K) and carbon dioxide adsorption isotherms of **1** at 273 K and 760 torr (CO₂: wine; N₂: purple; filled shapes: adsorption; open ones: desorption).

As shown in Fig. 3, owing to the porous nature of the framework, **1** can uptake considerable amounts of CO₂ at 273 K (18.7 cm³·g⁻¹). It is the first sample was characterized by adsorption isotherms with this kind of ligand and zinc metal. However, it is worth noting that almost no N₂ was adsorbed due to its smaller quadrupole moment than CO₂ (N₂: -4.7×10^{-40} Cm², CO₂: -1.4×10^{-39} Cm²).¹⁰ Unfortunately, the frameworks **2** was collapsed when guest molecules were vacuated from the frameworks, in addition, even the SCD was used, the framework of **1** was partially collapsed (Fig. S2, ESI). Compared with **1**, this phenomenon may be attributed to the extended ligand size of **2**, which made the framework unstable.

Conclusion

In summary, two porous Zn-MOFs with large solvent-accessible volume have been synthesized based on T-shaped pyridyl dicarboxylate linkers and zinc(II) salts. In the structure of **1**, there is tubular channel while there is Zn-(COO)-Zn chain in the structure of **2**. The different structures of them showed that the length and freedom of ligand play important roles in the construction of the frameworks. N₂ and CO₂ gas adsorption investigations show that **1** has permanent pores when the guests are evacuated.

Acknowledgements

This work was supported by Talent Cultivation Fund of

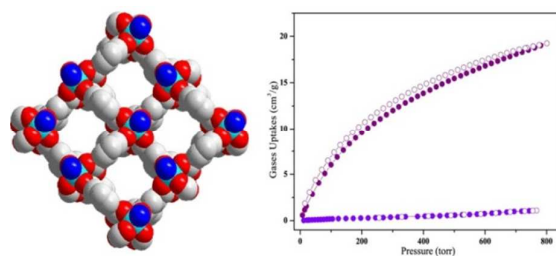
Anhui Normal University, the Doctoral Scientific Research Foundation and the Natural Science Foundation of Anhui Province 1408085ME83.

Appendix A. Supplementary data

Supplementary material CCDC 946740 and 946741 contain the supplementary crystallographic data for **1** and **2**. These data can be obtained free of charge from The Cambridge Crystallographic Centre via www.ccdc.cam.ac.uk/data-request/cif.

Notes and references

- (a) O. M. Yaghi, M. O'Keeffe, N. W. Ockwig, H. K. Chae, M. Eddaoudi, J. Kim, *Nature* 2003, **423**, 705; (b) K. Sumida, D. L. Rogow, J. A. Mason, T. M. McDonald, E. D. Bloch, Z. R. Herm, T.-H. Bae, J. R. Long, *Chem. Rev.* 2012, **112**, 724-781; (c) L. E. Kreno, K. Leong, O. K. Farha, M. Allendorf, R. P. V. Duyne, J. T. Hupp, *Chem. Rev.* 2012, **112**, 1105; (d) J. Duan, M. Higuchi, R. Krishna, T. Kiyonaga, Y. Tsutsumi, Y. Sato, Y. Kubota, M. Takata, S. Kitagawa, *Chem. Sci.* 2014, **5**, 660-666.
- (a) B. S. Zheng, R. R. Yun, J. Bai, Z. Y. Lu, L. T. Du, Y. Z. Li, *Inorg. Chem.* 2013, **52**, 2823; (b) K. Z. Tang, R. R. Yun, Z. Y. Lu, L. T. Du, M. X. Zhang, Q. Wang, H. Y. Liu, *Cryst. Growth&Des.* 2013, **13**, 1382; (c) S. N. Wang, R. R. Yun, Y. Q. Peng, Q. F. Zhang, J. Lu, J. M. Dou, J. Bai, D. C. Li, D. Q. Wang, *Cryst. Growth&Des.* 2012, **12**, 79; (d) Z. X. Wang, B. S. Zheng, H. T. Liu, X. Lin, X. Y. Yu, P. G. Yi, R. R. Yun, *Cryst. Growth&Des.* DOI: 10.1021/cg401180r; (e) Z. X. Wang, B. S. Zheng, H. T. Liu, P. G. Yi, X. F. Li, X. Y. Yu, R. R. Yun, *Dalt. Trans.* 2013, **42**, 11304.
- (a) R. R. Yun, J. G. Duan, J. Bai, Y. Z. Li, *Cryst. Growth Des.* 2013, **13**, 24; (b) R. R. Yun, Z. Y. Lu, Y. Pan, X. Z. You, J. Bai, *Angew. Chem. Int. Ed.* 2013, **52**, 11282.
- (a) Y. B. Zhang, H. L. Zhou, R. B. Lin, C. Zhang, Jian. B. Lin, J. P. Zhang, X. M. Chen, *Nat. Commun.* 2012, **3**, 642; (b) G. S. Papaefstathiou, L. R. MacGillivray, *Angew. Chem. Int. Ed.* 2002, **41**, 2070; (c) T. Ohmura, A. Usuki, K. Fukumori, T. Ohta, M. Ito, K. Tatsumi, *Inorg. Chem.* 2006, **45**, 7988; (d) Q. Wei, Nieuwenhuyzen, S. L. James, *Micro. Meso. Mat.* 2004, **73**, 97.
- (a) G. M. Sheldrick, SHELXS-97, Program for the Solution of Crystal Structures, University of Göttingen, Göttingen (Germany) 1997. See also: Sheldrick GM *Acta Crystallogr. A* 1990, **46**, 467; (b) G. M. Sheldrick, SHELXL-97, Program for the Refinement of Crystal Structures, University of Göttingen, Göttingen (Germany) 1997. See also: G. M. Sheldrick, *Acta Crystallogr. A* 2008, **64**, 112.
- A. L. Spek, *J. Appl. Crystallogr.*, 2003, **36**, 7.
- V. A. Blatov, M. V. Peaskov, *Acta Crystallogr. Sect. B* 2006, **62**, 457.
- <http://rcsr.anu.edu.au/>
- van der Sluis P, A. L. Spek, *Acta Crystallogr. A* 1990, **46**, 194.
- R. L. Amey, *J. Phys. Chem.* 1974, **78**, 1968.



The existence of nano-tubular channels in structure of **1** is responsible practically for moderate carbon dioxide uptakes at 273 K.